Scripta Materialia 182 (2020) 99–103

Contents lists available at ScienceDirect

Scripta Materialia

journal homepage: www.elsevier.com/locate/scriptamat

Influence of non-magnetic Cu on enhancing the low temperature magnetic properties and Curie temperature of FeCoNiCrCu(x) high entropy alloys

Varun Chaudhary[a], Vishal Soni[c], Bharat Gwalani[c,1], R.V. Ramanujan[a,b], Rajarshi Banerjee[c,*]

[a] School of Materials Science and Engineering, Nanyang Technological University, Singapore 639798, Singapore
[b] Singapore and Singapore-HUJ Alliance for Research and Enterprise (SHARE), Nanomaterials for Energy and Energy-Water Nexus (NEW), Campus for Research Excellence and Technological Enterprise (CREATE), Singapore 138602, Singapore
[c] Department of Materials Science and Engineering, University of North Texas, Denton, TX 76201, USA

ARTICLE INFO

Article history:
Received 22 December 2019
Accepted 21 February 2020

Keywords:
High entropy alloys
Magnetic materials
Curie temperature
Atom probe tomography

ABSTRACT

The microstructure and magnetic properties of three face-centered cubic (FCC) FeCoNiCrCu(x) high entropy alloys (HEAs) ($x = 0, 0.5, 1$) are investigated. Interestingly, addition of the nonmagnetic element Cu to FeCoNiCr HEA is found to enhance exchange interactions and low temperature saturation magnetization. The paramagnetic to ferromagnetic Curie transition temperature increases from 85 K for FeCoNiCr to 118 K for FeCoNiCrCu. This is counterintuitive since Cu is nonmagnetic; however, atom probe tomography revealed Cu rich clusters containing 5 at% Ni and 1 at% each of Fe, Co, Cr, within FCC matrix, these clusters altered the matrix composition and consequently its magnetic properties.

High-entropy alloys (HEAs) have recently attracted considerable attention, largely due to their unique combination of structural and physico-chemical properties. Consequently, conventional alloys may be replaced by HEAs in certain applications [1–6]. The formation of intermetallic compounds is quite common in conventional multi-component alloys. However, in the case of HEAs which contain multiple principal elements, random solid solutions are often stabilized. HEAs can possess many attractive physical and mechanical properties, hence they can be used for structural and functional applications as well as high hardness and wear resistant coatings [2,5,7]. This combination of excellent physical properties of HEAs offers applications such as tools, molds, dies, mechanical parts, structural components, and furnace parts [5,8].

The stability of a single phase solid solution in HEAs can be affected by many factors, such as mixing configurational entropy, atomic size misfit, mixing enthalpy etc. [3]. Some HEAs exhibit phase instability, e.g., elemental segregation, precipitation or spinodal decomposition [1]. Elemental segregation in HEAs influences configurational entropy, Gibbs free energy and physical properties. While FeCoNiCrCu HEAs deposited films were found to be single-phase solid solutions [3,9], they show significant elemental segregation of Cu in the bulk form. The four component FeCoNiCr alloy has been previously studied [2,10]. However, there is not much literature on the addition of the nonmagnetic element, Cu, to such alloys and its effect on magnetic properties.

Wang, et al. [11] investigated the magnetic properties of the HEA system, $CoCrCuFeNiTi_x$, varying the Ti content from $x = 0$ to 1. However, this paper does not discuss the influence of varying Cu on the magnetic and structural properties of these alloys. The composition $x = 0$ (CoCrCuFeNi) is similar to one of the samples investigated in the present study, however, it should be noted that the magnetic properties of $CoCrCuFeNiTi_x$ and CuxCrCoNiFe are totally different due to the difference in magnetic ordering of Ti (paramagnetic) and Cu (diamagnetic).

A recent computational study based on density function theory (DFT) by Huang et al. [12] discussed the influence of adding Cu to FeCoNiCr This paper reports an increase in the computed value of the Curie temperature (T_c) with Cu addition to FeCoNiCr. Unfortunately, the detail of exchange interaction values for FeCoNiCr and FeCoNiCrCu have not been reported in this paper and additionally the role of nonmagnetic Cu in increasing the Curie temperature has not been discussed in detail in this paper. The authors have assumed either an FCC or BCC solid solution phase in their calculations, while the experimental results of the present study show that the Cu containing FeCoNiCr samples exhibit two FCC phases, without any BCC phases, which can account for the difference in the T_c.

In the present study, we report the magnetic properties of three HEAs, FeCoNiCrCu(x) ($x = 0$, 0.5 and 1) and the correlation be-

* Corresponding author.
E-mail addresses: varun004@e.ntu.edu.sg (V. Chaudhary), rajarshi.banerjee@unt.edu (R. Banerjee).
[1] now at Pacific Northwest National Laboratory.

https://doi.org/10.1016/j.scriptamat.2020.02.037
1359-6462/

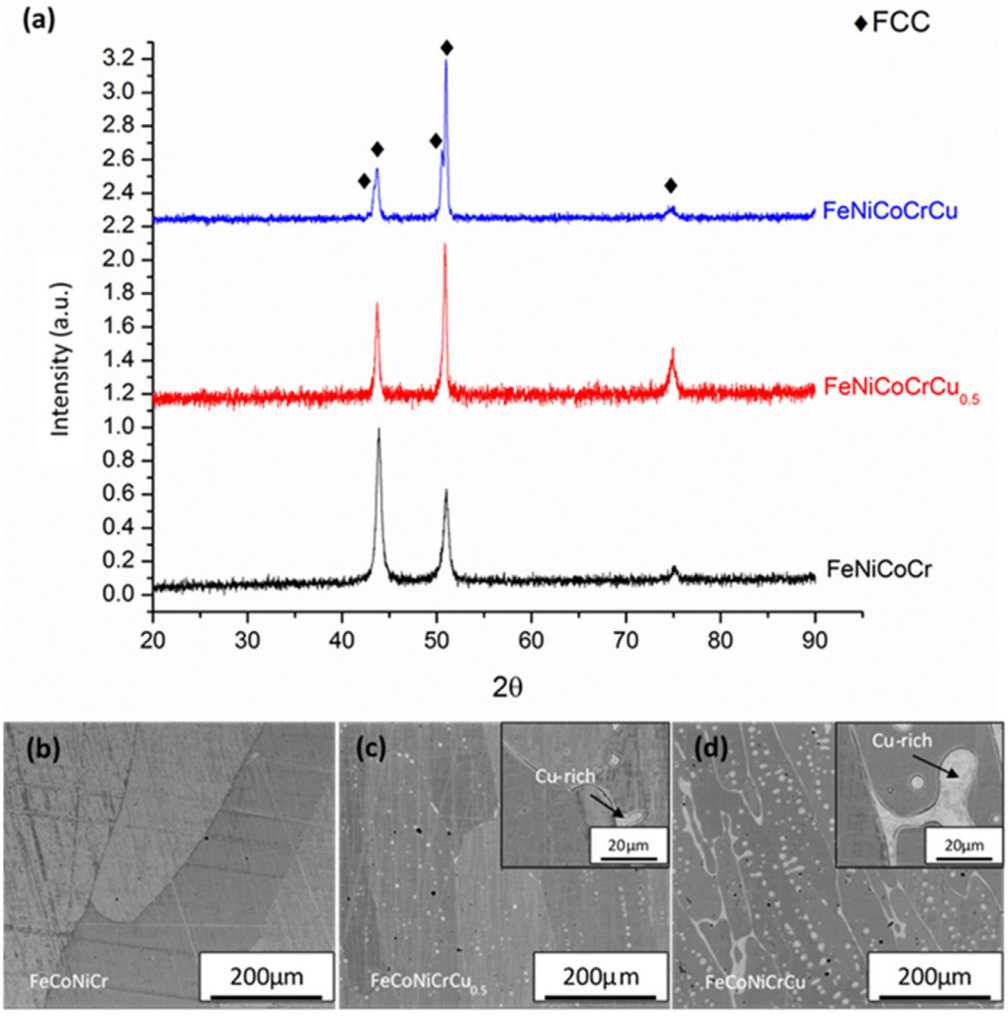

(e)

Alloy	Phase	Fe	Co	Ni	Cr	Cu
FeCoNiCr	Bulk	24.9	26.4	26.1	24.6	-
FeCoNiCr Cu0.5	Matrix	22.0	23.9	23.3	20.2	10.6
	Cu-rich phase	2.7	2.5	6.5	2.	86.0
FeCoNiCr Cu	Matrix	21.8	23.3	22.4	19.0	13.5
	Cu-rich phase	2.7	2.5	7.0	2.1	85.7

Fig. 1. (a) X-ray diffraction patterns and (b–d) SEM-back scattered electron diffraction images from FeNiCoCrCu(x) (x = 0, 0.5, 1) alloys. (e) Table showing the phase compositions (wt%) after solutionizing at 1200 °C for 30 min.

tween these properties and the microstructure. Interestingly, our results show enhanced low temperature ferromagnetic behavior and a higher Curie temperature (T_c) due to the addition of non-magnetic Cu to FeNiCoCr. This effect can be attributed to the formation of Cu clusters in the HEAs, resulting in a Cu rich and Cu lean two phase system.

FeCoNiCrCu(x) (x = 0, 0.5 and 1) HEAs were prepared by arc melting of elemental Fe, Co, Ni, Cr and Cu pellets (99.9% purity) under argon atmosphere. The resulting buttons were annealed at 1200 °C for 30 min under argon and subsequently quenched in water. The phase analysis of samples was performed using a Rigaku Ultima III X-ray diffractometer, using CuKα radiation. The composition and microstructures were characterized by a SEM, using a FEI Nova-NanoSEM 230^{TM} coupled with an energy dispersive x-ray spectrum analyzer. Standard lift-out techniques were followed for Atom Probe Tomography (APT) sample preparation using a FEI Nova 200 dual beam focused ion beam (FIB). APT experiments were conducted on a CAMECA local electrode atom probe 3000X HR instrument. All experiments were performed in the temperature range of 20–40 K with target evaporation of 0.5%. The magnetic properties were measured using a PPMS (EverCool-II, QD), equipped with a vibrating sample magnetometer probe.

The as-cast alloys of the three compositions were solutionized at 1200 °C/30 min followed by water quenching. Fig. 1(a) shows the X-ray diffraction patterns obtained from these FeCoNiCrCu(x) (x = 0, 0.5 and 1) alloys. It can be seen that the FeNiCoCr and

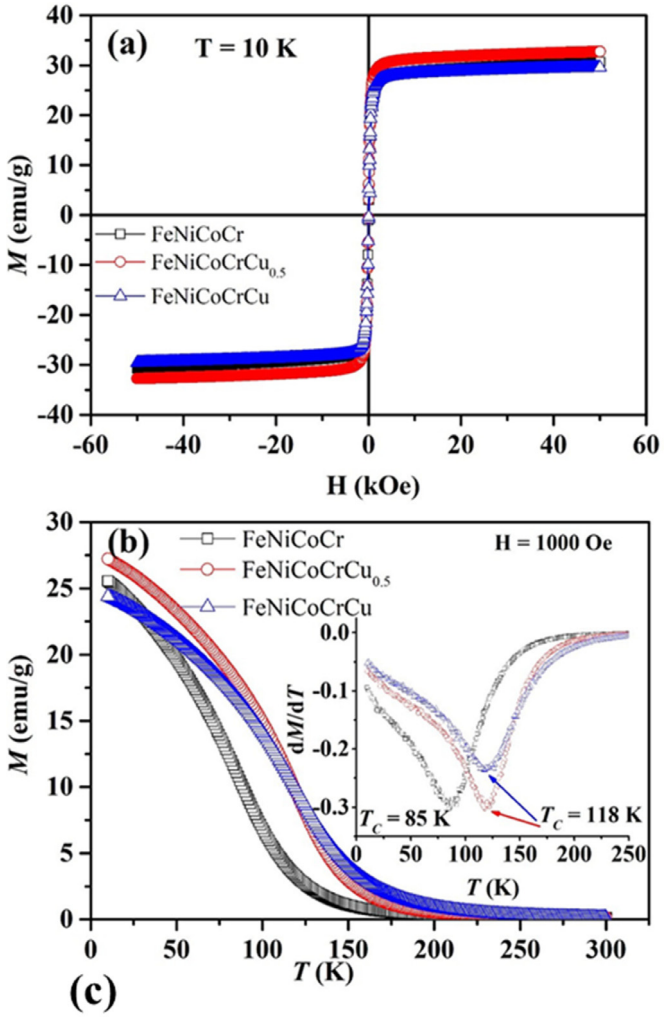

HEAs	M_S (emu/g)	H_C (Oe)	T_c (K)
FeCoNiCr	30.7	23	85
FeCoNiCrCu$_{0.5}$	32.7	33	118
FeCoNiCrCu	29.6	33	118

Fig. 2. (a) Magnetization (M) versus applied magnetic field (H) at 10 K for FeNiCoCr, FeCoNiCrCu$_{0.5}$ and FeCoNiCrCu. (b) M versus T at a magnetic field of 1000 Oe, inset of (b) shows the rate of change of magnetization with respect to temperature. (c) Table showing the Saturation magnetization (M_S) and coercivity (H_C) measured at 10 K, as well as Curie temperature (T_c) values for FeCoNiCrCu(x) (x = 0, 0.5 and 1).

FeNiCoCrCu$_{0.5}$ alloys appear to be single phase FCC solid solutions whereas the FeNiCoCrCu alloy consists of two FCC phases. However, backscattered SEM images (Fig. 1(b–d)) from these alloys revealed that two FCC phases were present in both Cu containing alloys, i.e., FeNiCoCrCu$_{0.5}$ and FeNiCoCrCu. The FCC matrix phase and a Cu-rich inter-dendritic phase can be seen in the inset of Fig. 1(c) and (d). Cu segregation is expected in these alloys due to the large positive enthalpy of mixing between Fe–Cu, Co–Cu and Cr–Cu. Fig. 1(e) shows a table consisting of the compositions of the matrix and the Cu-rich phase in these alloys obtained by SEM-EDS. For both CoCrFeNiCu$_{0.5}$ and CoCrFeNiCu alloys, only ~10 wt% of Cu dissolves in the matrix.

Fig. 2(a) shows the magnetic hysteresis loops obtained at 10 K for FeNiCoCrCu(x) (x = 0, 0.5 and 1). FeNiCoCrCu(x) will exhibit Fe–Fe, Fe–Co, Fe–Ni, Ni–Ni, Ni–Co and Co–Co nearest neighbour exchange interactions between the ferromagnetic components.

The exchange interactions beyond the next-nearest neighbor sites are expected to be weekly distributed. Antiferromagnetic exchange interactions result from the interaction of Cr with Fe, Ni, Cr and Co. Cu is a non-magnetic transition metal component, which has negligible or weak Ruderman–Kittel–Kasuya–Yosida (RKKY) coupling to the ferromagnetic components. When the Cu content increases from 0 to 0.5, the saturation magnetization (M_S) increased from 30.7 emu/g to 32.7 emu/g. Zuo et al., also reported enhanced M_S, when Al (or Ga) was introduced in the CoFeMnNi [6]. When the value of x in FeNiCoCrCu(x) increases to 1, M_S decreased because the Cu content in matrix for x = 0.5 and 1 are similar (as can be seen from the SEM results). Cu in the second phase does not enhance ferromagnetic interactions. The coercivities (H_C) of the samples for x = 0.5 and 1 are higher than the corresponding value for Cu free samples. The value of H_C for FeCoNiCr was found to be 23 Oe, while the H_C of both FeCoNiCrCu$_{0.5}$ and FeCoNiCrCu were 33 Oe.

Fig. 2(b) shows the temperature dependence of magnetization of FeCoNiCrCu(x) HEAs, measured upon cooling from 300 K to 10 K, under a field of 1 kOe. All the samples exhibit paramagnetic behavior at room temperature. It was previously reported that FeCoNiCr is paramagnetic at room temperature [10,13] but there is no report of the temperature dependence of magnetization of FeCoNiCrCu HEAs. The T_c of FeCoNiCr was 85 K, whereas both the Cu containing alloys, i.e., FeCoNiCrCu$_{0.5}$ and FeCoNiCrCu, exhibit Tc of 118 K, as determined from the minima of the plot of dM/dT versus T (inset of Fig. 2(b)). It is interesting that in addition to an increase in configurational entropy, Tc also increases by addition of Cu to FeNiCoCr alloys. The T_c of FeNiCoCrCu$_{0.5}$ and FeNiCoCrCu is similar because both alloys have similar Cu content in the matrix. Although elemental Cu is nonmagnetic, it can increase positive exchange interactions between other atoms due to magnetovolume effects [14]. Fig. 2(c) shows the M_S and H_C measured at a temperature 10 K and Tc for FeCoNiCrCu$_x$ (x = 0, 0.5 and 1).

The FeCoNiCrCu$_{0.5}$ alloy exhibited unusual higher values of M_S and T_c compared to the FeCoNiCr alloy, and was therefore selected for detailed analysis using APT. The aim was to determine the distribution of alloying elements, especially Cu, within the fcc matrix of this alloy. Fig. 3(a) shows the individual ion maps of Fe, Co, Ni, Cr and Cu from a FeNiCoCrCu$_{0.5}$ alloy. It can be clearly seen from the ion maps that Cu clusters form within the fcc matrix. These Cu clusters exhibit a size range from ~3 to ~5 nm. A proximity histogram or proxigram analysis across the FCC matrix/Cu-clusters interface based on an iso-concentration surface (isosurface) corresponding to 40-at% Cu, separating the matrix region from the Cu-clusters, is shown in Fig. 3(b). It is to be noted that a proximity histogram is a unique method to determine the composition across a precipitate-matrix interface, selected using an iso-concentration surface. This proxigram is generated by probing compositional variations at every point perpendicular to the above-mentioned interface. The composition profiles, in the form of proximity histograms across a 40 at% Cu isosurface, have been plotted in Fig. 3(b). Cu-rich clusters are primarily composed of Cu (~92at%) and Ni (~5at%) together with ~1 at% each of Fe, Co, and Cr. Fig. 3(c) shows the Cu ion map from a APT reconstruction exhibiting different sizes of Cu clusters. A 1-D compositional profile across three Cu clusters of different sizes reveals that the composition of the clusters is influenced by their size, i.e. the bigger clusters have more Cu content than the smaller ones. Additionally, it should be noted that even after the formation of these Cu-rich clusters, the fcc solid solution matrix retains an average Cu content of approximately 5at%, based on the proximity histogram (composition profile) for Cu shown in Fig. 3(b).

Referring to the DFT-based computational study by Huang et al. [12], their computed T_c value for the fcc solid solution phase in-

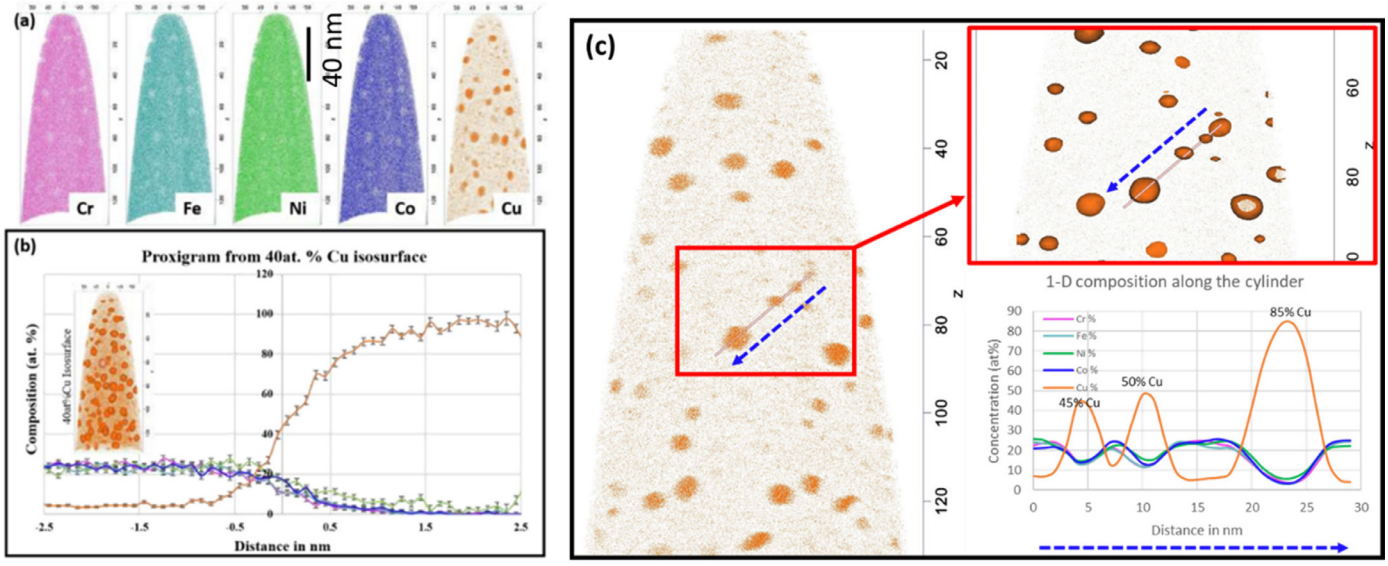

Fig. 3. Atom probe tomography (a) elemental ion maps of Cr, Fe, Ni, Co and Cr from $FeNiCoCrCu_{0.5}$ alloy (b) Proximity histogram profiles showing the compositional partitioning of FCC matrix and Cu rich cluster. (c) APT reconstruction showing Cu ion map with a blow up of the clusters having different sizes (top right) and a 1-D compositional profile across three clusters of different sizes.

creased from 155 K in case of FeCoNiCr to 251 K for FeCoNiCrCu. The results of present study indicate that the T_c value of the FeCoNiCr single phase fcc solid solution is 85 K, and it increases to 118 K for both Cu containing $FeCoNiCrCu_{0.5}$ and FeCoNiCrCu alloys. It should be noted that in the case of both the Cu containing alloys, the fcc matrix composition is nominally the same, and contains 4.5–5 at%Cu, while the remaining Cu in these alloys resides in the Cu-rich clusters within the fcc matrix (Fig. 3) and macroscopic Cu-rich interdendritic regions in between the fcc dendrites (refer to Fig. 1(b)). Interestingly, the fcc solid solution matrix composition in the case of both of the Cu containing alloys is approximately $FeCoNiCrCu_{0.2}$. Based on the previously reported DFT calculations [10], the computed increase in the T_c value of the fcc solid solution phase from FeCoNiCr to FeCoNiCrCu is 96 K. Since the experimental results indicate that the actual composition of the fcc solid solution phase is $FeCoNiCrCu_{0.2}$, the weighted fractional increase in the T_c value, based on the DFT computations, is expected to be 20 K. Interestingly, the experimentally observed increase in the T_c value of both Cu containing alloys is 33 K, are in good agreement with the computed value.

Additionally, the Cu-rich nanoclusters within the fcc matrix can influence the T_c value. Cu-rich clusters are primarily composed of Cu (~92 at%) and Ni (~5at%) together with ~1 at% each of Fe, Co, and Cr. The higher Ni content in the Cu-rich clusters results in a reduction of Ni content within the fcc matrix. Consequently, the fcc matrix has a higher level of Co and Fe, leading to an increase in positive exchange interactions within the matrix, thus increasing the T_c of the alloy.

The T_c of FeCoNiCrCu is less than that of the reported value of T_c (400 K) for FeCoNiMnCu [15]. This difference can be understood from the mean field model value of $Tc = J(r)_{eff} Z_T S(S + 1)/3k_B$, where $J(r)_{eff}$ is the effective exchange interaction, Z_T is coordination number, S is the atomic spin quantum number and kB is the Boltzmann constant. $J_{Cr\text{-}Cr}$ has a more negative value than $J_{Mn\text{-}Mn}$. Hence, $J(r)_{eff}$ for FeCoNiCrCu is less than the $J(r)_{eff}$ for FeCoNiMnCu, resulting in lower Tc. Tunable Curie temperatures are of high interest [15–17]. These $FeCoNiCrCu_x$ based HEAs are useful for magnetocaloric applications in which the service temperature is ~100 K. They are cheaper than recently reported HEAs for magnetocaloric applications [18]. Fig. 4 shows a comparison of T_c of the alloys investigated in the present study with other reported values

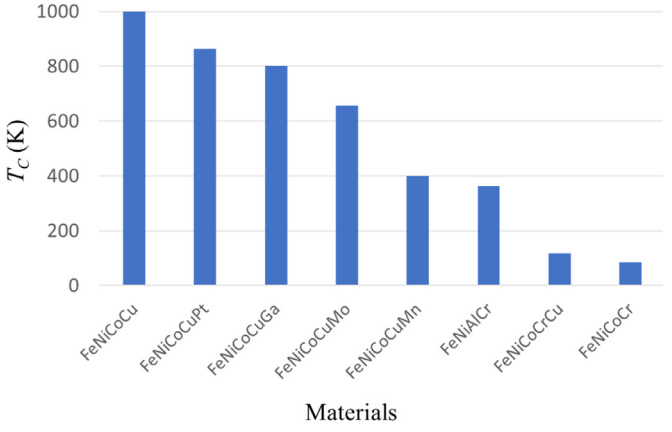

Fig. 4. Curie temperature of FeNiCoCu, FeNiCoCuPt, FeNiCoCuGa, FeNiCoCuMo, FeNiCoCuMn [15], FeNiAlCr, FeNiCoCrCu, FeNiCoCr high entropy alloys.

of T_c for different HEAs [15]. It can be seen that the T_c of HEAs can be tuned in a large range from ~100 K to well above room temperature. The $FeCoNiCrCu_x$ alloys exhibit T_c below room temperature which can be used for the magnetocaloric applications where service temperature ~100 K. Additionally the $FeCoNiCrCu_x$ based alloys are more cost effective than recently reported HEAs for magnetocaloric applications [18,19]. The T_c can be tuned to near room temperature by decreasing Cr concentration or increasing Co content in $FeCoNiCrCu_x$ based HEAs.

Addition of nonmagnetic Cu enhances low temperature saturation magnetization in FeNiCoCrCu(x) alloys. A paramagnetic to ferromagnetic transition occurs at Curie temperatures (T_c) of 85 K and 118 K for FeCoNiCr and $FeCoNiCrCu_x$ ($x = 0.5$ and 1.0) alloys, respectively. The increase in T_c in the Cu containing alloys can be rationalized to the following effects:

1. Previously reported DFT-based computations clearly indicated that the addition of Cu to the fcc matrix of FeCoNiCr leads to an increase in the T_C. The experimentally measured increase in the T_c in the present study is in good agreement with the DFT results.

2. APT investigations revealed that some of the Cu does not dissolve in the fcc FeCoNiCr solid solution, but instead forms ~3–5 nm sized Cu-rich clusters homogeneously distributed within the fcc matrix. The presence of Ni in these Cu-rich clusters resulted in a reduction of Ni in the fcc matrix, leading to an indirect increase in the Tc in these alloys.

Declaration of Competing Interest

The authors declare that they have no known competing financial interests or personal relationships that could have appeared to influence the work reported in this paper.

Acknowledgements

The authors would like to acknowledge the Materials Research Facility (MRF) at UNT for access to advanced characterization facilities. This research is partially supported by the National Research Foundation, Prime Minister's Office, Singapore under its Campus for Research Excellence and Technological Enterprise (CREATE) program.

References

[1] Y.F. Ye, Q. Wang, J. Lu, C.T. Liu, Y. Yang, Mater. Today 19 (6) (2016) 349–362.
[2] M.-.H. Tsai, Entropy 15 (12) (2013) 5338.
[3] Y.F. Ye, Q. Wang, Y.L. Zhao, Q.F. He, J. Lu, Y. Yang, J. Alloy. Compd. 681 (2016) 167–174.
[4] V. Chaudhary, B. Gwalani, V. Soni, R.V. Ramanujan, R. Banerjee, Sci Rep 8 (1) (2018) 15578.
[5] T. Borkar, V. Chaudhary, B. Gwalani, D. Choudhuri, C.V. Mikler, V. Soni, T. Alam, R.V. Ramanujan, R. Banerjee, Adv. Eng. Mater. 19 (8) (2017) 1700048.
[6] T. Zuo, M.C. Gao, L. Ouyang, X. Yang, Y. Cheng, R. Feng, S. Chen, P.K. Liaw, J.A. Hawk, Y. Zhang, Acta Mater. 130 (2017) 10–18.
[7] Y.J. Zhou, Y. Zhang, Y.L. Wang, G.L. Chen, Appl. Phys. Lett. 90 (18) (2007) 181904.
[8] Y. Zhang, T.T. Zuo, Z. Tang, M.C. Gao, K.A. Dahmen, P.K. Liaw, Z.P. Lu, Prog. Mater. Sci. 61 (2014) 1–93.
[9] Z. An, H. Jia, Y. Wu, P.D. Rack, A.D. Patchen, Y. Liu, Y. Ren, N. Li, P.K. Liaw, Mater. Res. Lett. 3 (4) (2015) 203–209.
[10] M.S. Lucas, L. Mauger, J.A. Muñoz, Y. Xiao, A.O. Sheets, S.L. Semiatin, J. Horwath, Z. Turgut, J. Appl. Phys. 109 (7) (2011) 07E307.
[11] X.F. Wang, Y. Zhang, Y. Qiao, G.L. Chen, Intermetallics 15 (3) (2007) 357–362.
[12] S. Huang, E. Holmström, O. Eriksson, L. Vitos, Intermetallics 95 (2018) 80–84.
[13] Y.-.F. Kao, S.-.K. Chen, T.-.J. Chen, P.-.C. Chu, J.-.W. Yeh, S.-.J. Lin, J. Alloy. Compd. 509 (5) (2011) 1607–1614.
[14] P. Gorria, D. Martínez-Blanco, J.A. Blanco, A. Hernando, J.S. Garitaonandia, L. Fernández Barquín, J. Campo, R.I. Smith, Phys. Rev. B 69 (21) (2004) 214421.
[15] M. Kurniawan, A. Perrin, P. Xu, V. Keylin, M. McHenry, IEEE Magn. Lett. 7 (2016) 1–5.
[16] V. Chaudhary, R.V. Ramanujan, Sci. Rep. 6 (2016) 35156.
[17] V. Chaudhary, X. Chen, R.V. Ramanujan, Prog. Mater. Sci. 100 (2019) 64–98.
[18] Y. Yuan, Y. Wu, X. Tong, H. Zhang, H. Wang, X.J. Liu, L. Ma, H.L. Suo, Z.P. Lu, Acta Mater. 125 (2017) 481–489.
[19] D.D. Belyea, M.S. Lucas, E. Michel, J. Horwath, C.W. Miller, Sci. Rep. 5 (2015) 15755.